Exact Diagonalization Studies of 2D Quantum Models

D. Poilblanc
Laboratoire de Physique des Solides
Université Paris-Sud
91405 Orsay, France

Abstract: A review on recent calculations of various equal-time and dynamical correlations of the 2-dim. t-J and frustrated Heisenberg models by Lanczos diagonalizations of small clusters is given. In particular, the existence of uniform or staggered chiral order is questioned by calculating both static or dynamical correlations of a *plaquette* chiral operator. The plaquette-plaquette correlation falls off rapidly with distance and, hence, no evidence is found for long range chiral order. However, our numerical results reveal increasing chiral fluctuations at low energy upon doping in the t-J model or upon increasing frustration in the Heisenberg model. On the other hand, the dimer phase appears as a serious candidate for a disordered phase in the intermediate J_2/J_1-region of the frustrated Heisenberg model. Twisted boundary conditions are used to calculate the optical conductivity of the t-J model. The Drude weight is deduced from the curvature of the energy surface in the parameter space of the twist angles. In the range $1/8 < J/t < 0.5$ the Drude weight is almost independent on the ratio J/t and corresponds to a mass enhancement of ~ 3. Our numerical work also reveals a remarquably large optical absorption in the frequency range $0 < \omega < 3t$ and, typically, less than 40% of the total optical weight is left in the Drude peak (at $\omega = 0$). At small J/t, both Drude weight and finite frequency absorption scale almost linearly with doping. These results are discussed in connection with the optical experiments in the High-T_c cuprates.

1 Introduction

A common feature of most non-conventional theories of superconductivity[1, 2] is the occurence of time reversal symmetry breaking (TRSB) involving the flux condensation of a topological gauge field. Alternatively, unusual transport properties of the "normal phase" of the High-T_c superconductors have been explained by large fluctuations of the gauge field.[3] First, we wish to study, by using numerical methods,[4, 5, 6] the possible occurence of such phenomena in two simple 2D models believed to contain the *minimal* ingredients for either TRSB or large gauge field fluctuations to take place.

The first candidate is the frustrated Heisenberg model defined as,

$$\mathcal{H} = J_1 \sum_{\mathbf{i},\vec{\epsilon}} \mathbf{S_i} \cdot \mathbf{S_{i+\vec{\epsilon}}} + J_2 \sum_{\mathbf{i},\vec{\delta}} \mathbf{S_i} \cdot \mathbf{S_{i+\vec{\delta}}}, \tag{1}$$

where $\mathbf{i}$ denotes the sites of a 2D square lattice, $\vec{\epsilon}$ are the two unit vectors along the x or y directions and $\vec{\delta}$ are vectors along the diagonal of the plaquettes. $\mathbf{S_i}$ are spin 1/2 operators. In the limits $J_2 << J_1$ and $J_1 << J_2$ one expects an antiferromagnetic (Néel) state and a collinear state (with alternating parallel rows or columns of up and down spins) respectively. On the other hand, in the intermediate range $J_2/J_1 \sim 1/2$, according to mean-field theory,[7] frustration would lead to a chiral spin liquid phase exhibiting TRSB.

*Laboratoire associé au CNRS

In contrast to the previous model, the frustration in the t-J model is created dynamically by holes which perturb the antiferromagnetic spin background;

$$\mathcal{H} = J\sum_{\mathbf{i},\vec{\epsilon}}(\mathbf{S_i}\cdot\mathbf{S_{i+\vec{\epsilon}}} - \frac{1}{4}n_{\mathbf{i}}n_{\mathbf{i}+\vec{\epsilon}}) - t\sum_{\mathbf{i},\vec{\epsilon},\sigma}(\tilde{c}^{\dagger}_{\mathbf{i},\sigma}\tilde{c}_{\mathbf{i}+\vec{\epsilon},\sigma} + h.c.). \tag{2}$$

where $\tilde{c}^{\dagger}_{\mathbf{i},\sigma} = (1-n_{\mathbf{i},-\sigma})c^{\dagger}_{\mathbf{i},\sigma}$ and $c^{\dagger}_{\mathbf{i},\sigma}$ and $n_{\mathbf{i},\sigma}$ are the fermion creation operator and the fermion density at site $\mathbf{i}$, respectively. The $t-J$ model is widely believed to give the simplest description of the low energy physics of the "normal phase" of the High-T_c cuprates. Therefore, besides the study of the chiral fluctuations, we shall also investigate the nature of the optical conductivity in this model. This issue is addressed in section 3.

The numerical results presented below are obtained by exact diagonalizations (Lanczos algorithm) of small $N = 4\times 4$ clusters with periodic (section 2) or twisted (section 3) boundary conditions. For the t-J model one ($N_h = 1$) or two ($N_h = 2$) holes are considered.

2 Chiral Correlations

2.1 Static Correlations

To study chirality in the ground state (GS) or chiral fluctuations we define a chiral operator like

$$O_{pl}(\mathbf{Q}) = \frac{1}{N}\sum_{\mathbf{i}}\exp(i\mathbf{Q}\cdot\mathbf{i})\,O^{A_2}_{\mathbf{i}}, \tag{3}$$

where the plaquette operator reads,

$$\begin{aligned} O^{A_2}_{\mathbf{i}} &= \mathbf{S_i}\cdot(\mathbf{S_{i+x}}\times\mathbf{S_{i+x+y}})\,n_{\mathbf{i+y}}, \\ &+ \mathbf{S_{i+x}}\cdot(\mathbf{S_{i+x+y}}\times\mathbf{S_{i+y}})\,n_{\mathbf{i}}, \\ &+ \mathbf{S_{i+x+y}}\cdot(\mathbf{S_{i+y}}\times\mathbf{S_i})\,n_{\mathbf{i+x}}, \\ &+ \mathbf{S_{i+y}}\cdot(\mathbf{S_i}\times\mathbf{S_{i+x}})\,n_{\mathbf{i+x+y}}. \end{aligned} \tag{4}$$

The momenta $\mathbf{Q} = \mathbf{0}$ (uniform) and $\mathbf{Q} = (\pi,\pi)$ (staggered) are here of particular interest. According to group theory, O_{pl} is a *singlet* operator of A_2 spatial symmetry, i.e. *odd* under axis reflections (parity or P), and is even under $\pi/2$-rotation. O_{pl} is also *odd* under time reversal (T) since it defines a sign of circulation around the plaquettes. A very similar plaquette operator $O^{B_1}_{\mathbf{i}}$ odd under $\pi/2$-rotation and even under axis reflections can be constructing by using appropriate phase factors in 4 (see Fig. 1a for the related correlation function) but only $O^{A_2}_{\mathbf{i}} \neq 0$ in a chiral (TRSB) ground state.

In the $J_1 - J_2$ model, we shall consider the competition with the dimer state, in which the spins are coupled in singlet bonds forming columns. For this state, a relevant order parameter can be defined as,

$$\begin{aligned} \mathcal{O}_{dim} &= \frac{1}{N}\sum_{\mathbf{i}}\mathcal{O}^{dim}_{\mathbf{i}}, \\ \text{where}\quad \mathcal{O}^{dim}_{\mathbf{i}} &= \frac{1}{2}((-1)^{i_x}\,\mathbf{S_i}\cdot\mathbf{S_{i+\hat{x}}} - (-1)^{i_x}\,\mathbf{S_i}\cdot\mathbf{S_{i-\hat{x}}} \\ &\quad + i\,(-1)^{i_y}\,\mathbf{S_i}\cdot\mathbf{S_{i+\hat{y}}} - i\,(-1)^{i_y}\,\mathbf{S_i}\cdot\mathbf{S_{i-\hat{y}}}). \end{aligned} \tag{5}$$

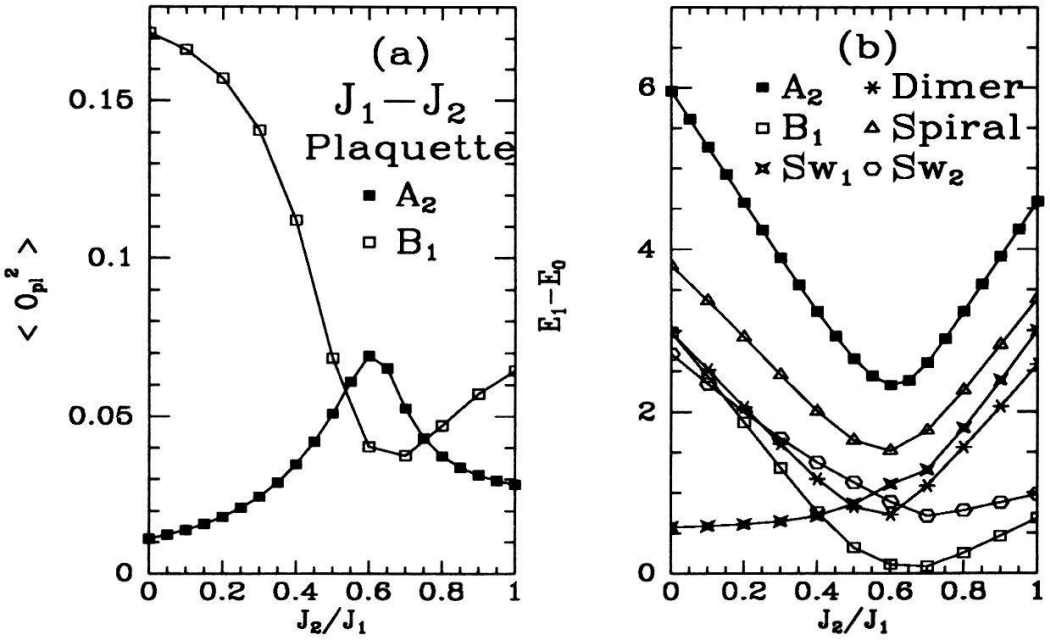

Fig. 1: *(a) Uniform correlation functions; (b) energy gaps for different symmetries.*

The equal-time correlations $\langle O_{pl}^2(\mathbf{Q}=\mathbf{0})\rangle$ in the frustrated Heisenberg model in Fig. 1a reveals a significant increase of the chiral correlation for the A_2 symmetry of the plaquette operator and for intermediate $J_2/J_1 \sim 0.5$. Although this suggests that frustration may favor chiral ordering, (i) short distance effects are usually important in finite cluster calculations and (ii) different disordered phases like the dimer phase may also compete with the chiral liquid phase.

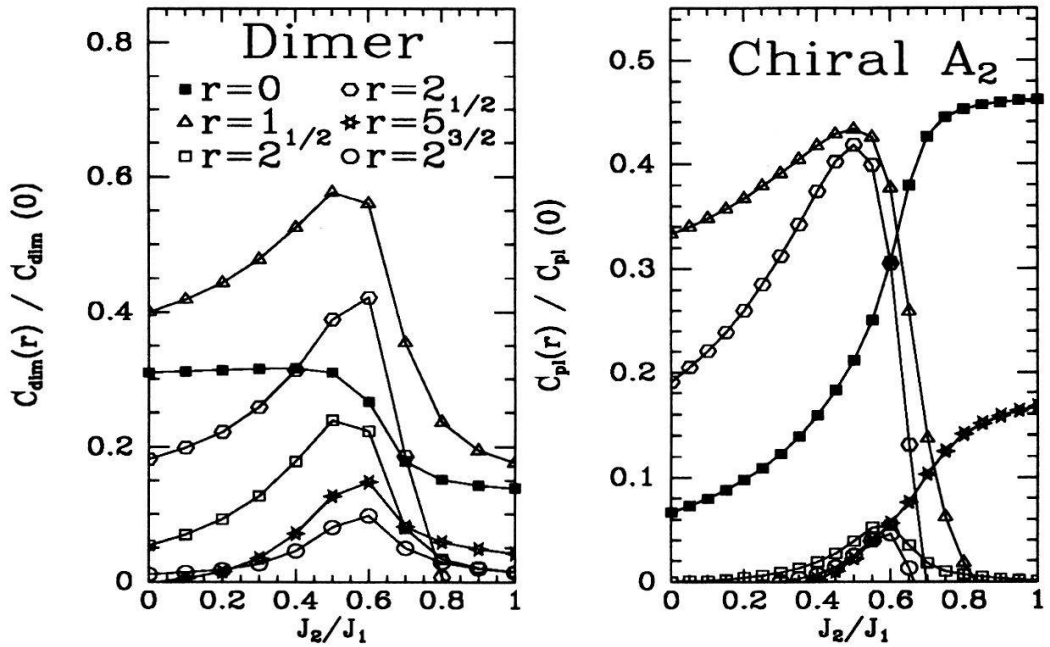

Fig. 2: *Dimer and chiral (plaquette-plaquette) correlation functions* $C_\alpha(\mathbf{0})$ $(\mathbf{r}=\mathbf{0})$ *and* $C_\alpha(\mathbf{r})/C_\alpha(\mathbf{0})$ *at various distances in the* J_1-J_2 *model*

Therefore it is also required to study correlation functions with distance like

$$C_{pl}(\mathbf{r}) = \frac{1}{2N} \sum_{\mathbf{i}} \langle O^{A_2}_{\mathbf{i}+\mathbf{r}} O^{A_2}_{\mathbf{i}} + O^{A_2}_{\mathbf{i}} O^{A_2}_{\mathbf{i}+\mathbf{r}} \rangle. \tag{6}$$

One can also define[4] a similar correlation function $C_{dim}(\mathbf{r})$ associated with dimer order (for which the spins are coupled in singlet bonds forming columns). Fig. 2 shows comparative plots of these correlation functions. The on-site correlation $\langle (O^{A_2}_{\mathbf{i}})^2 \rangle$ gives in fact a large contribution to the correlation function $\langle O^2_{pl} \rangle$. However, Fig. 2 reveals a small enhancement of the chiral correlations at the largest distances available in the intermediate-J_2/J_1 region. In the case of the dimer operator the enhancement is significantly larger so that dimer order seems to be a better candidate for a disordered phase. Larger cluster calculations are clearly needed in order to give a more definite conclusion.[8]

Let us now turn to the discussion of the t-J model. As shown in Fig. 3, the equal-time correlation $\langle O^2_{pl} \rangle$ at $\mathbf{Q} = \mathbf{0}$ depends weakly on the doping or on the ratio t/J. On the other hand, the *staggered* correlation is enhanced by a large hole kinetic energy. At large doping fractions and $t/J > 5$ the staggered component even exceeds the uniform one.

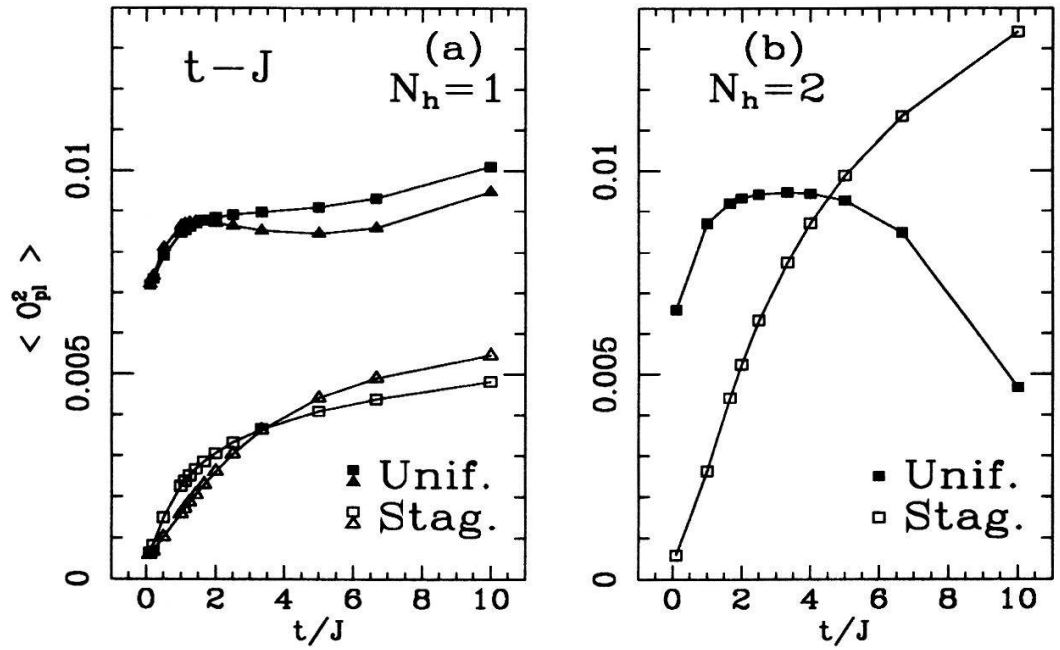

Fig. 3: *Uniform (closed symbols) and staggered (open symbols) plaquette correlation function* $\langle O^2_{pl} \rangle$ *in a* 4×4 *cluster of the t-J model.* $(\pi/2, \pi/2)$ *(squares) and* $(\pi, 0)$ *(triangles) one hole-GS momenta have been considered.*

However, for all dopings studied, the plaquette-plaquette correlation (6) is found to fall off rapidly with distance. If long range order exists, we then expect a small value $\langle O_{pl} \rangle \leq 0.04$ for the order parameter.

2.2 Dynamical Correlations

Although, it is probable that long range chiral order does not exist, strong chiral (or gauge field) fluctuations would play a very important role.[3] In order to study such fluctuations we consider the spectral representation of O_{pl} (uniform),

$$I_{pl}(\omega) = \sum_n |\langle \psi_n | O_{pl} | \psi_0 \rangle|^2 \delta(\omega + E_0 - E_n), \tag{7}$$

where $|\psi_n\rangle$ are eigenstates of $\mathcal{H}$ with energy E_n ($E_0 < E_n, n > 0$).

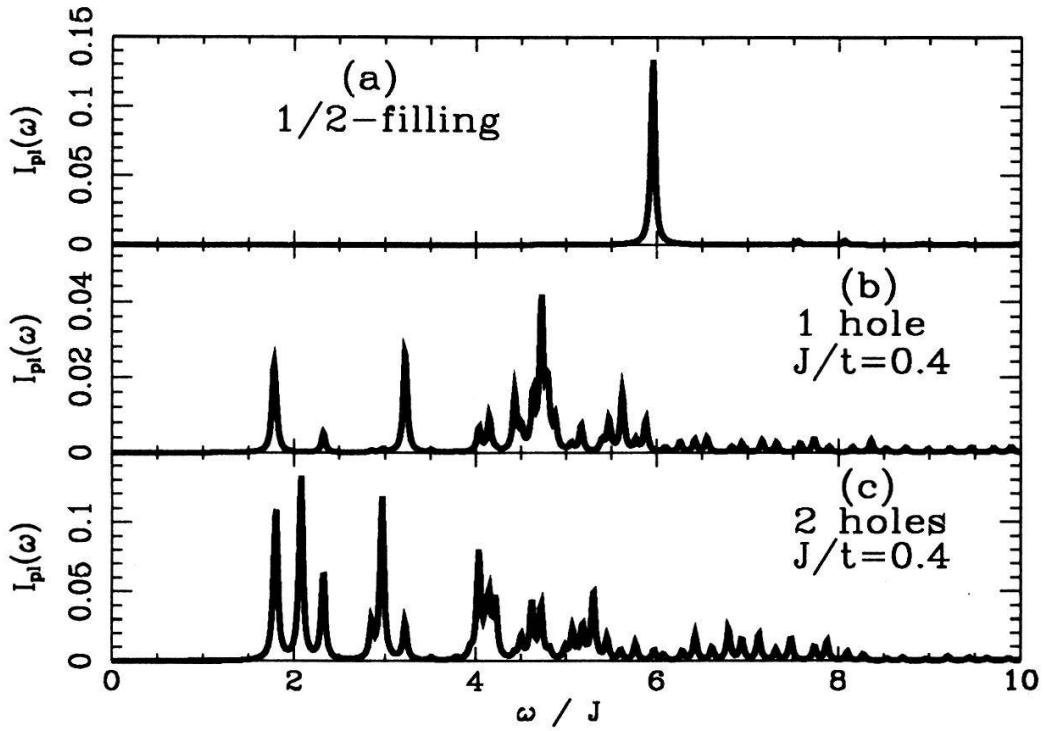

Fig. 4: *Dynamical chiral correlation function at* $\mathbf{Q} = \mathbf{0}$ *calculated on a* 4×4 *cluster with various hole numbers.*

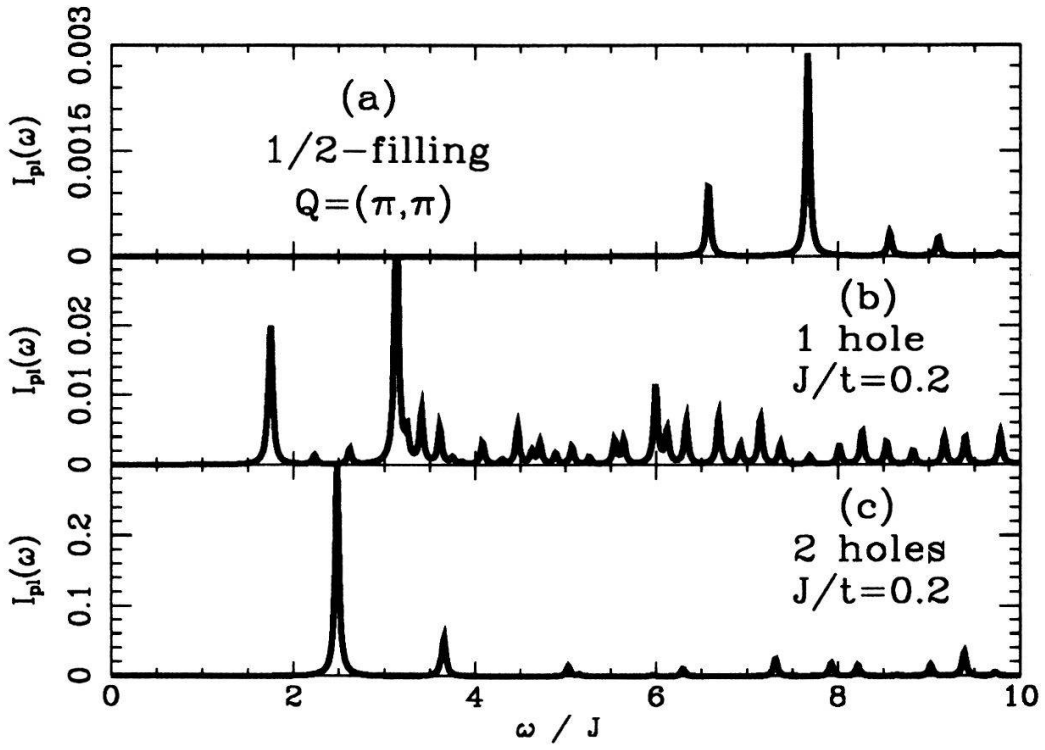

Fig. 5: *Dynamical chiral correlation function at* $\mathbf{Q} = (\pi, \pi)$ *calculated on a* 4×4 *cluster.*

For the $J_1 - J_2$ model, $O_{pl}(\mathbf{Q} = \mathbf{0})$ induces transitions from the singlet fully symmetric GS $|\psi_0\rangle$ to the singlet A_2 excited states (odd under parity). The effect of the frustration J_2 is simply to shift the very sharp feature of Fig. 4a (Heisenberg model with $J_2 = 0$) to lower energy. In the thermodynamic limit one would expect the spectrum to become broader but small cluster calculations probably give the right estimate for the average position of the peak. The behavior of the gap (refered as A_2) associated with the lowest energy transition versus J_2/J_1 is shown in Fig. 1b. In fact, whatever J_2/J_1, triplet states characteristic of $\mathbf{Q} = \mathbf{0}$ (Sw1) or $\mathbf{Q} = (\pi, 0)$ (Sw2) spin-wave excitations ($S^+_{\mathbf{Q}} \mid \Psi_0\rangle$) or of a spiral (twisted) state stay always below the lowest A_2 state (Fig. 1b). We point out that, in the intermediate-J_2/J_1 region, the four lowest energy states (including the GS) are singlet states (Fig. 1b) that are compatible with a four-fold degenerate dimer state in the thermodynamic limit. Indeed, by linear combinations of the four dimer configurations (parallel rows of dimer bonds and equivalent configurations obtained by translation and/or rotation), one can straightforwardly construct (i) a $\mathbf{Q} = \mathbf{0}$ totally symmetric (A_1) state, (ii) a $\mathbf{Q} = \mathbf{0}$ state odd under $\frac{\pi}{2}$-rotation (B_1), (iii) two non-uniform $(\pi, 0)$ and $(0, \pi)$-momentum states. Hence, the gaps refered as "B_1" and "dimer" in Fig. 1b can be interpreted as the corresponding splittings between these states which are expected to occur in a finite size system.

In contrast to the frustrated Heisenberg model, when dynamical frustration through holes ($t-J$ model) is introduced, the spectral decomposition of O_{pl} becomes much broader, as seen from Fig. 4. It is interesting to note that spectral weight is transfered to lower energy. These low-energy fluctuations of the plaquette chiralities can alternatively be viewed as gauge field fluctuations[3] , typical of strongly correlated systems. However, spinwave-like ($S = 1$) excitations still exist at lower energies. For example, at $J/t = 0.4$ and $N_h = 2$, a sharp spinwave peak occurs at $\omega \sim 0.7J$ in the spin fluctuation spectrum while the lowest A_2 $S = 0$ excited state lies around $1.75J$ (Fig. 4). Comparing uniform (Fig. 4) and staggered (Fig. 5) chiral fluctuation spectra we have found that more spectral weight is concentrated at low energy in the staggered case.

We finish this section by a comment about spiral correlations in the $t - J$ model. To study this order we define the vector operator

$$\mathbf{T_i} = \mathbf{S_i} \times (\mathbf{S_{i+x}} + \mathbf{S_{i+y}}), \tag{8}$$

and its associated correlation $\mathcal{O}_{\mathrm{spi}} = < \frac{1}{N} (\sum_{\mathbf{i}} \mathbf{T_i})^2 >$. We have also observed that $\mathcal{O}_{\mathrm{spi}}$ is slightly enhanced (of about 25% with respect to half-filling) at small doping and small ratio J/t.[6] However, this enhancement occurs in a regime where the spin correlations are strongly suppressed (except at short distances) by the hole motion. We then conclude that there is no real evidence for a long range incommensurate phase, although a local twist between spins at short distances may occur.[9]

3 Optical Conductivity in the t-J Model

In this section, we turn to the calculation of the optical conductivity of the $t - J$ model. This issue is closely related to the concept of charge stiffness which characterizes the response of a finite size system to a change in the boundary conditions (BC).[10] To implement arbitrary BC, the hopping term in (2) is multiplied by a phase factor according to

$$\tilde{c}^\dagger_{\mathbf{i},\sigma} \tilde{c}_{\mathbf{i}+\vec{\epsilon},\sigma} \rightarrow \tilde{c}^\dagger_{\mathbf{i},\sigma} \tilde{c}_{\mathbf{i}+\vec{\epsilon},\sigma} \exp(i\vec{\epsilon} \cdot \vec{\kappa}), \tag{9}$$

where $\vec{\kappa} = 2\pi(\frac{\phi_x}{L_x}\vec{x} + \frac{\phi_y}{L_y}\vec{y})$ and $L_\alpha (= 4)$ are the lenghts of the cluster. Since the system is topologically equivalent to a torus, these phases can alternatively be seen as the result of two fluxes ϕ_x and ϕ_y inserted through the two holes of the torus. For example, $\phi_\alpha = 0$ $(= 1/2)$ corresponds

to periodic (antiperiodic) BC. The GS energy $\tilde{E}(\vec{\kappa})$ is obtained by the Lanczos method and is generally made of several intersecting branches.[11] Since $\tilde{E}(\vec{\kappa})$ is a periodic function of the fluxes, we shall restrict ourselves to $-1/2 \leq \phi_\alpha \leq 1/2$.

The real part of the optical conductivity reads

$$Re\,\sigma_{\alpha\alpha}(\omega,\vec{\kappa}) = 2\pi D_{\alpha\alpha}(\vec{\kappa})\,\delta(\omega) + \sigma^{reg}_{\alpha\alpha}(\omega,\vec{\kappa}), \tag{10}$$

where the regular part is proportional to the spectral function of the current-current correlation function,

$$\sigma^{reg}_{\alpha\alpha}(\omega,\vec{\kappa}) = \frac{\pi}{N|\omega|}\sum_{m\neq 0} |\langle\Psi_m \mid j_\alpha \mid \Psi_0\rangle|^2\,\delta(|\omega| - E_m + \tilde{E}). \tag{11}$$

We emphasize here that in (11) both GS, excited states, energies and current operator $j_\alpha = \partial\mathcal{H}/\partial\kappa_\alpha$ depend on the twist $\vec{\kappa}$ in the BC. The Drude weight, term proportional to $\delta(\omega)$, is directly proportional to the local charge stiffness,[10]

$$D_{\alpha\beta}(\vec{\kappa}) = \frac{1}{2}\frac{\partial^2(\tilde{E}(\vec{\kappa})/N)}{\partial\kappa_\alpha\partial\kappa_\beta}. \tag{12}$$

The total weight at finite frequency, $\int d\omega\,\sigma^{reg}_{\alpha\alpha}$, is also of physical interest and will be compared to the Drude weight.

When $N \to \infty$, at fixed hole density, one expects that the BC (i.e. the value of $\vec{\kappa}$) will no longer play a role. However, in the case of a small 4×4 cluster, the local curvature tensor still depends on the choice of the BC. Finite size effects can be estimated by using various averaging weighting factors,

$$\langle D_{\alpha\beta}\rangle_{\phi_x,\phi_y} = \oint d\phi_x \oint d\phi_y\, W(\tilde{E}(\vec{\kappa}))D_{\alpha\beta}(\vec{\kappa}) \tag{13}$$

where $\oint$ means that the integral is performed over a period of the flux. The same procedure is also applied to the regular part of the conductivity

$$\langle\sigma^{reg}_{\alpha\alpha}\rangle_{\phi_x,\phi_y} = \oint d\phi_x \oint d\phi_y\, W(\tilde{E}(\vec{\kappa}))\,\sigma^{reg}_{\alpha\alpha}, \tag{14}$$

and the integrated finite frequency absorption $2\rho_0$,

$$2\rho_0 = \int d\omega\,\langle\sigma^{reg}_{\alpha\alpha}\rangle_{\phi_x,\phi_y}. \tag{15}$$

Practically, we have chosen two extreme limits (i) $W(\tilde{E}) = 1$ (that leads to a uniform average) or (ii) $W(\tilde{E}) = Z^{-1}\delta(\tilde{E} - \tilde{E}_0)$ (where Z is a normalization factor). In the second case, $\tilde{E}_0$ corresponds to the lowest energy of $\tilde{E}(\vec{\kappa})$ so that only the local curvatures at the energy minima are considered. What are the actual locations of the absolute minima? It is interesting to note that, in general, $\vec{\kappa} = \mathbf{0}$ (i.e. periodic BC) do not correspond to the absolute minimum of the energy but rather to a local maximum or minimum. Indeed, restricting ourselves to $N_h = 2$ holes for simplicity (but the conclusions are qualitatively very similar for $N_h = 1$), we have found that, for $1/8 \leq J/t \leq 0.5$, the energy minima are located at $(\phi_x,\phi_y) = (0,\pm 1/2)$ and $(\pm 1/2, 0)$. For $J/t \geq 2/3$ the minima lie at $(\phi_x,\phi_y) = (\pm 1/2, \pm 1/2)$. When $J/t \to 0$, many crossings occur rapidly between the various branches indicating a transition towards a ferromagnetic phase. For example, at $J/t = 0.1$ the minima are located at $(\phi_x,\phi_y) = (\pm\phi_0, \pm\phi_0)$ ($\phi_0 \sim 0.284$) and for $J/t = 1/16$ at $(\phi_x,\phi_y) = \mathbf{0}$.[12]

At $J/t = 0$, the ferromagnetic state is optained for $(\phi_x, \phi_y) = (0, \pm 1/2)$ and $(\pm 1/2, 0)$. This more complex regime will be studied separately.[13]

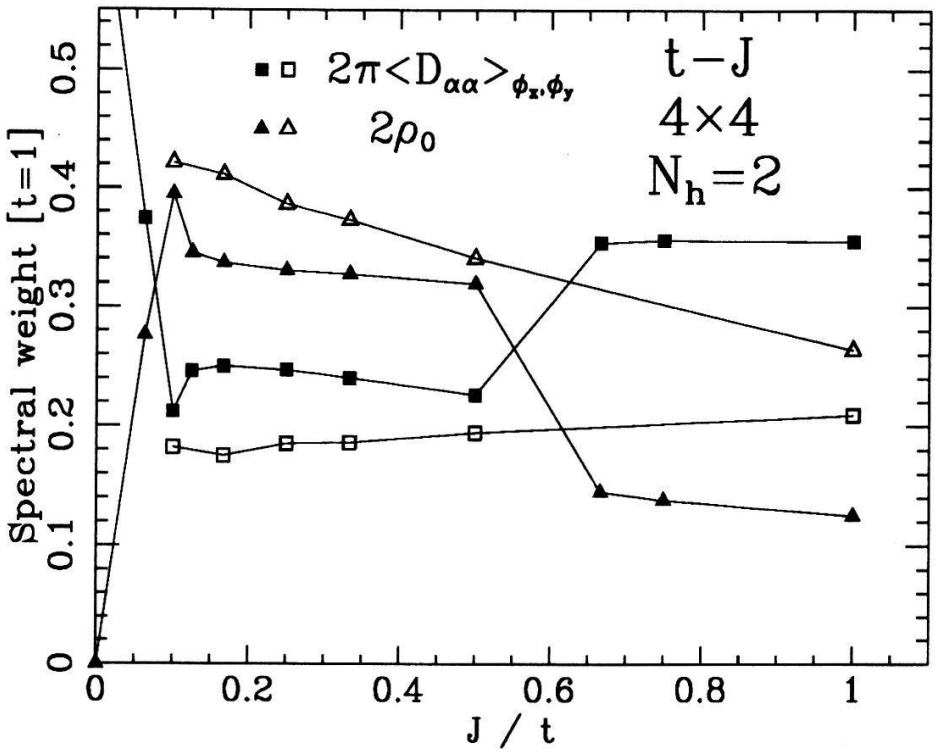

Fig. 6: *Drude weight and finite frequency optical absorption versus J/t. The open and closed symbols correspond to the two different choices (i) and (ii) respectively for the weighting factors (see text).*

The behavior of the Drude weight and the finite frequency absorption are shown on Fig. 6 versus J/t. Uniformly averaging the curvature $\tilde{E}(\vec{\kappa})$ over the twist $\vec{\kappa}$ gives a continuous curve with J/t (open symbols). On the other hand, the Drude weight and $2\rho_0$ calculated from the local curvatures at the minima of $E(\vec{\kappa})$ exhibit discontinuities at some particuliar values of J/t (for example between $J/t = 0.5$ and $2/3$) when a level crossing occurs between the bottom of two separate branches. However, we do not know yet whether such discontinuities indicate actual first order transitions in the infinite system (like e.g. a phase separation for large J/t[14]). Since the curvature of $\tilde{E}(\vec{\kappa})$ is larger at the minima the two averaging procedures give, roughly speaking, a lower and a upper bound for the Drude weight. In the range $0.1 < J/t < 0.5$, these two values are resonnably close (within 20%) so that this method can give quantitative predictions. First, we should notice that the Drude weight is rather unsensitive to the ratio J/t, (at least in the range 0.1-0.5). Compared to the ferromagnetic value $2\pi\langle D^F_{\alpha\alpha}\rangle \sim 0.67$ (for $N_h = 2$ and $J/t = 0$) we obtain a typical ratio of $\langle D_{\alpha\alpha}\rangle / \langle D^F_{\alpha\alpha}\rangle \sim 0.3$ which corresponds to a mass enhancement of order 3. We also find that the Drude weight scale almost proportionally with doping. All these results are in qualitative agreement with slave boson treatments of the metallic phase.[15] For $J/t \geq 2/3$ we notice a sudden transfer of spectral weight from finite to zero frequency. This may well be the sign of an instability towards phase separation.[14]

Interestingly, our calculations show that the integrated weight $2\rho_0$ (Fig. 6) of the finite frequency conductivity (Fig. 7) is surprisingly large and even exceeds the Drude weight for $0.1 < J/t < 0.5$. This is to be connected to the anomalous mid-infrared absorption observed experimentally in the

high-T_c cuprates.[16]

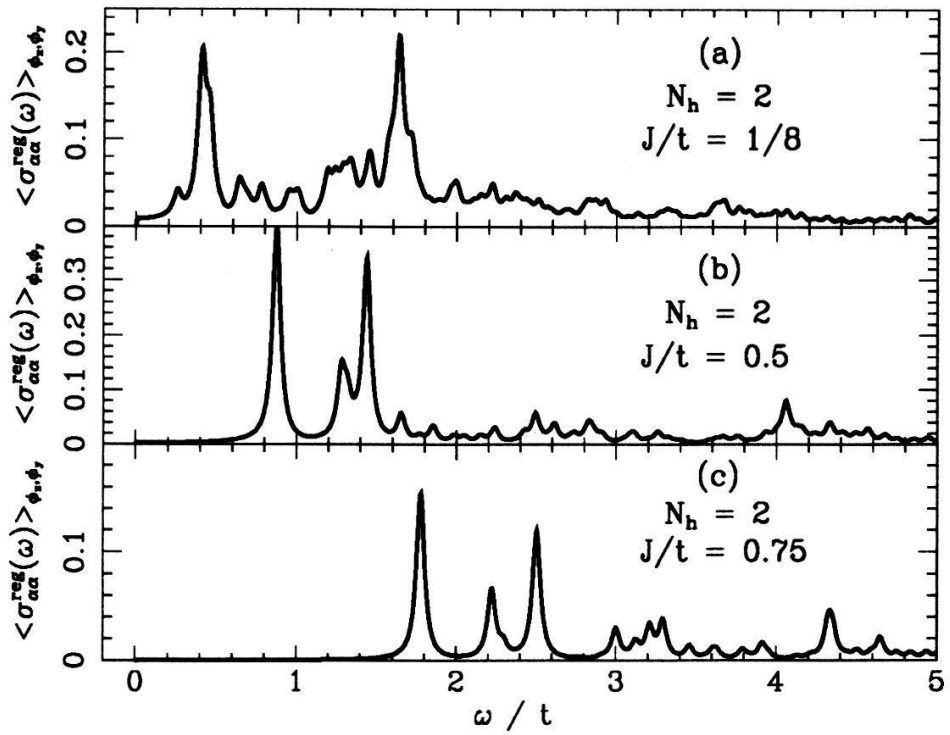

Fig. 7: *Regular part of the optical conductivity versus frequency for various values of J/t. The calulation is performed at the minima of $\tilde{E}(\vec{\kappa})$.*

As shown in Fig. 7, the main absorption occurs in the frequency range $0 < \omega < 3t$. For $1/8 < J/t < 0.5$ the mean-frequency $\overline{\omega}$ defined as the first moment of the spectrum,

$$\overline{\omega} = \int d\omega\, \omega \langle \sigma^{reg}_{\alpha\alpha} \rangle_{\phi_x,\phi_y} / 2\rho_0, \tag{16}$$

can be parametrized as $\overline{\omega} \sim 1.9t + 0.7J$ and depends only weakly on J. At $J/t \sim 2/3$ $\overline{\omega}$ jumps to $\sim 3.2t$ and reaches $\sim 3.9t$ at $J/t = 1$. These large values are characteristic of a tail $\sim 1/\omega$ extending to large energies.[17]

4 Conclusion

Our small cluster calculation reveals relatively short distance correlations of chirality between plaquettes. This means that, if long range chiral order exists, the order parameter must be very small. In the $J_1 - J_2$ model, the dimer phase is a serious candidate for a disordered phase competing with the PT-breaking phase. In the t-J model, the hole kinetic energy seems to favor *staggered* chiral correlations rather than uniform. In both models, low energy chiral fluctuations are enhanced by frustration. However only dynamical frustration by holes leads to a large broadening of the fluctuation spectrum.

We have also calculated the optical conductivity in the t-J model by twisting the boundary conditions. The spectrum exhibits interesting level crossings as a function of the twist. The Drude weight is deduced from the curvature of the energy surface at the bottom of the spectrum and is found to depend only weakly on the ratio J/t. The Drude weight is reduced by approximately a factor 3 with respect to the ferromagnetic state (which occurs at $J = 0$). Our work also reveals

a surprisingly large optical weight in the frequency range $0 < \omega < 3t$ which we identify with the observed mid-infrared absorption in the high-T_c copper oxides.

Acknowledgments

This project was supported in part by the EEC Science Program. The computer simulations were done on the CRAY-YMP at the San Diego Supercomputer Center, San Diego, California and on the CRAY-2 of Centre de Calcul Vectoriel pour la Recherche, Palaiseau, France. We thank SDSC and CCVR for their support.

References

[1] R.B. Laughlin, Phys. Rev. Lett. **60**, 2677 (1988).

[2] P. Lederer, D. Poilblanc, T.M. Rice, Phys. Rev. Lett. **63**, 1519 (1989).

[3] I.B. Ioffe and A.I. Larkin, Phys. Rev. B **39**, 8988 (1989); N. Nagaosa and P.A. Lee, Phys. Rev. Lett. **64**, 2450 (1990).

[4] D. Poilblanc, E. Gagliano, S. Bacci, E. Dagotto, Phys. Rev. B **43**, 10 970 (1991) and references cited therein.

[5] D. Poilblanc, E. Dagotto, J. Riera, Phys. Rev. B **43**, 7899 (1991) and references cited therein.

[6] E. Dagotto, A. Moreo, F. Ortolani, D. Poilblanc, J. Riera, D. Scalapino, NSF-ITP-91-54 preprint (1991).

[7] X.G. Wen, F. Wilczek, and A. Zee, Phys. Rev. B **39**, 11413 (1989).

[8] Surprisingly, a finite size scaling analysis of the gaps in the fluctuation spectra of the 4×4 and the 6×6 clusters seems to indicate that both dimer and chiral phases are stable in the vicinity of $J_2/J_1 \sim 1/2$ (see H. Schulz and T. Ziman, Orsay preprint (1991)).

[9] B. Shraiman and E. Siggia, Phys. Rev. Lett. **62**, 1564 (1989).

[10] W. Kohn, Phys. Rev. **133**, A171 (1964).

[11] D. Poilblanc, E. Dagotto, Phys. Rev. B **44**, 466 (1991); D. Poilblanc, Phys. Rev. B **44**, under press (1991).

[12] In this case ($J/t = 1/16, \vec{\kappa} = \mathbf{0}$) the GS is a totally symmetric A_1 spin singlet (S=0).

[13] D. Poilblanc et al. (in preparation).

[14] V. Emery, S. Kivelson, and H. Lin, Phys. Rev. Lett. **64**, 475 (1990).

[15] M. Grilli, G. Kotliar, Phys. Rev. Lett. **64**, 1170 (1990); see also J.P. Rodriguez, Orsay preprint.

[16] G.A. Thomas et al. Phys. Rev. B **40**, 11358 (1989) and references cited therein.

[17] T. M. Rice and F. C. Zhang, Phys. Rev. B **39**, 815 (1989).